The Spontaneous Aiming Mechanism of Magnetic Islands to the Pellets in tokamaks

M. Li[1], X. Y. Yang[1], A. H. Mao[1], D. Hu[2], X. G. Wang[1], C. Chen[1], X. Z. Yin[1], Z. P. Yang[1]

[1] *School of physics, Harbin Institute of Technology, Harbin 150001, China*

[2] *School of physics, Beihang University, Beijing 100191, China*

1 Introduction

Disruptions are a major threat to tokamak operation because they can produce severe thermal loads, electromagnetic forces, and runaway-electron risks [1]. Shattered pellet injection (SPI) is an effective disruption mitigation technique and is considered as the reference concept for the ITER disruption mitigation system [2]. Previous studies have shown that SPI can enhance impurity radiation, redistribute stored plasma energy, and excite magnetohydrodynamic (MHD) activity [3–5].

However, the interaction between SPI and pre-existing finite magnetic islands has not been fully clarified. Since tearing modes (TMs) are toroidally periodic while pellet injection is strongly localized, this interaction is intrinsically three-dimensional. In this work, three-dimensional nonlinear simulations are performed with the CLT code to investigate the response of a pre-existing (m/n=2/1) magnetic island to SPI. The results reveal that the island can spontaneously reorient toward the pellet injection location before the pellet reaches the resonant surface.

2 Simulation Setup

The simulations are performed using the three-dimensional nonlinear reduced MHD code CLT. The pellet is introduced through a density source term in the continuity equation, while the associated cooling effect is included in the temperature equation:

$$\frac{\partial \rho}{\partial t} = -\nabla \cdot (\rho v) + \nabla \cdot (D_\perp \nabla \rho) + \nabla_\parallel \cdot (D_\parallel \nabla_\parallel \rho) + S \quad (1)$$

$$\frac{\partial T}{\partial t} = -v \cdot \nabla T - (\gamma - 1) T \nabla \cdot v + (\gamma - 1)[\nabla \cdot (\kappa_\perp \nabla T)] + \nabla_\parallel \cdot (\kappa_\parallel \nabla_\parallel T) - ST/\rho \quad (2)$$

where ρ and T denote the plasma density and temperature, respectively. The ablative density source $S(r, t)$ is given by a Gaussian shape distribution around the pellet with position (R_f, Z_f, ϕ_f), as defined in equation (3):

$$S(r,t) = S_0 T_e^{\frac{5}{3}} r_p^{\frac{4}{3}} n_e^{\frac{1}{3}} \cdot e^{-\frac{(R-R_f)^2+(Z-Z_f)^2}{\delta r_{NG}^2}} e^{-\frac{(\phi-\phi_f)^2}{\delta \phi_{NG}^2}} \quad (3)$$

where T_e is the electron temperature, n_e is electron density and r_p is the pellet radius. This formulation of the source term follows the Neutral Gas Shielding (NGS) ablation model proposed by Parks. The HL-2A tokamak equilibrium is used in this simulation work, in which the major and the minor radii are set to be R_0 = 1.65 m and a = 0.40 m. The safety factor q and pressure p profiles shown in Fig. 1(a). The pellet is injected from a normalized minor radius $r \approx 0.94$a with a velocity of 500 m/s. The initial parameters are set to r_{p0}=0.1 cm, δr_{NG}=3.4 cm and $\delta \Phi_{NG}$=0.2 rad.

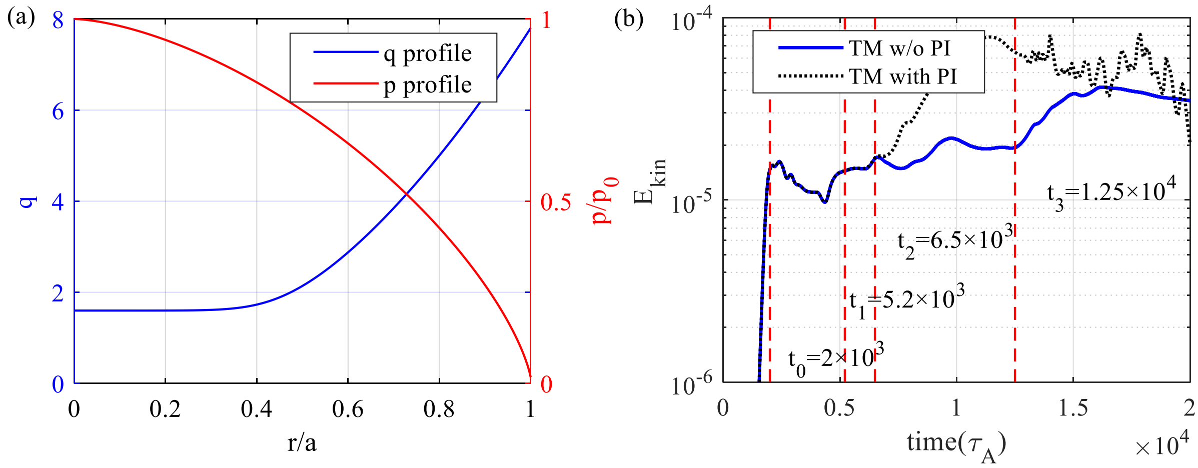

Fig. 1. (a) Initial equilibrium profiles of the safety factor *q*(r) and pressure *p*(r); (b) Time evolution of the perturbed kinetic energy E_K for the TM, with and without pellet injection.

3 Plasma response after pellet injection

As shown in Fig. 1(b), the TMs without pellet injected increase linearly at about $t_0 \sim 2 \times 10^3\ \tau_A$ and then saturate at a nonlinear level. As shown in Fig. 2(a–c), the pellet is injected at $t_1 \sim 5.2 \times 10^3\ \tau_A$, when the plasma is in the nonlinear stage of the *m*/*n*=2/1 TM, and magnetic islands have already developed. At $t_2 \sim 6.5 \times 10^3\ \tau_A$, the ablation cloud is deposited between the rational surfaces of *q*=4 and *q*=6, as shown in Fig. 2(d-f), and the local density is significantly higher than equilibrium. The major magnetic flux surfaces are kept well without obvious magnetic island structure changed. After $t_2 \sim 6.5 \times 10^3\ \tau_A$, the perturbed kinetic energy begins to increases and then reaches a peak in Fig. 1(b). At $t_3 \sim 1.25 \times 10^4\ \tau_A$, the pellet reaches the *q*=2 rational surface, the density along the pellet trace, and the perturbed density distributes inside *q*=5 rational surface due to toroidal propagation and rotation transformation. The 2/1 TM mode has no obvious change, but the 3/1, 4/1, and 4/2 modes are generated. The magnetic field lines are made stochastic and the closed flux surfaces and magnetic island structures of 2/1 and 3/1 modes are destroyed, on the other hand, magnetic islands with higher modes can be observed. In this process, the pellet excites TM instability, which subsequently leads to the destruction of confinement. This facilitates the release of magnetic energy during the disruption, thereby mitigating losses caused by the disruption. After the pellet passes the *q*=2 flux surface, pronounced amplitude oscillation emerges in the energy evolution and the TM begins to evolve highly nonlinearly. As shown in Figure 2(j-l), the pellet has been ablated and produces a higher density distribution in the core, the density perturbation forms a global structure with poloidal period distribution and radial phase shear. The magnetic surfaces and magnetic islands are restoring and the stochasticity decreases to its initial state. The amplitude of 2/1 perturbation decreases and disintegrates in radial direction, the other perturbation components also distribute along the whole radium.

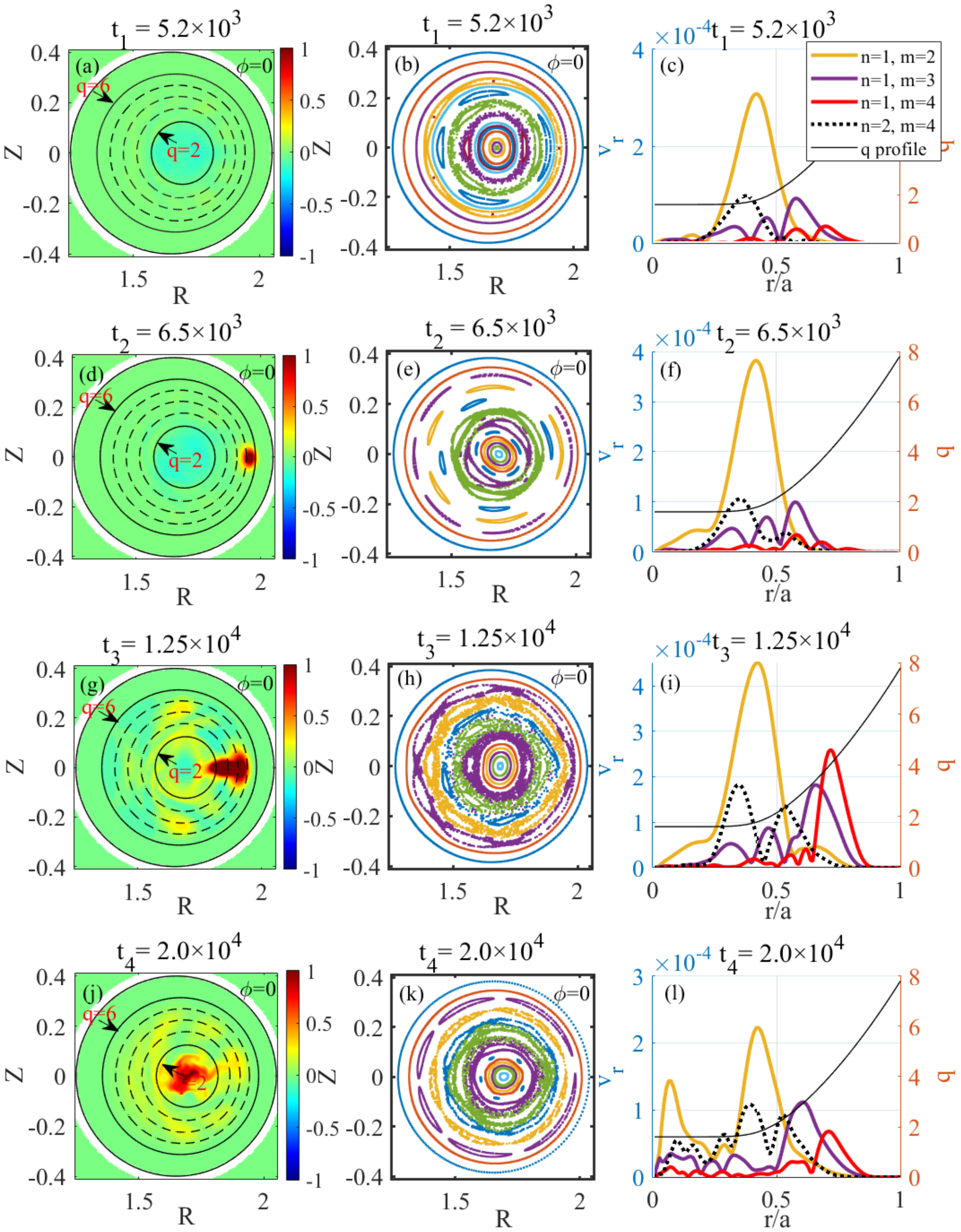

Fig. 2. The normalized perturbed density cross-section, Poincaré plots of the magnetic field lines, and amplitude profile of the perturbed radial velocity v_r, at (a)-(c) $t_1 \sim 5.2 \times 10^3\ \tau_A$, (d)-(f) $t_2 \sim 6.5 \times 10^3\ \tau_A$, (g)-(i) $t_3 \sim 1.25 \times 10^4\ \tau_A$, and (j)-(l) $t_4 \sim 2.0 \times 10^4\ \tau_A$, with pellet injection.

To make sure from which position is better to mitigate disruption damage, simulations are performed with the pellet injected at different toroidal positions, as shown in Fig. 3. Due to the toroidal symmetry, it is equivalent to changing the initial phases of the TM magnetic islands, which will be different for different toroidal positions. At $t_3 \sim 1.25 \times 10^4 \tau_A$, when the pellet reaches the q=2 rational surface, the TM mode structure are the same at the pellet inject cross section, even though the initial phase is different at $t_1 \sim 5.2 \times 10^3\ \tau_A$. This points out that no matter the pellet injected at the X-point or the O-point, the TM will respond to the pellet by rotating the magnetic island, ultimately causing the O-point to face the pellet. This indicates that the magnetic island can spontaneously reorient toward the pellet injection location, allowing the O-point to align with the localized pellet perturbation and generate a series of harmonic TM modes to release the magnetic energy. This suggests that the SPI injection phase does not require special consideration and make the pellet injection more robust.

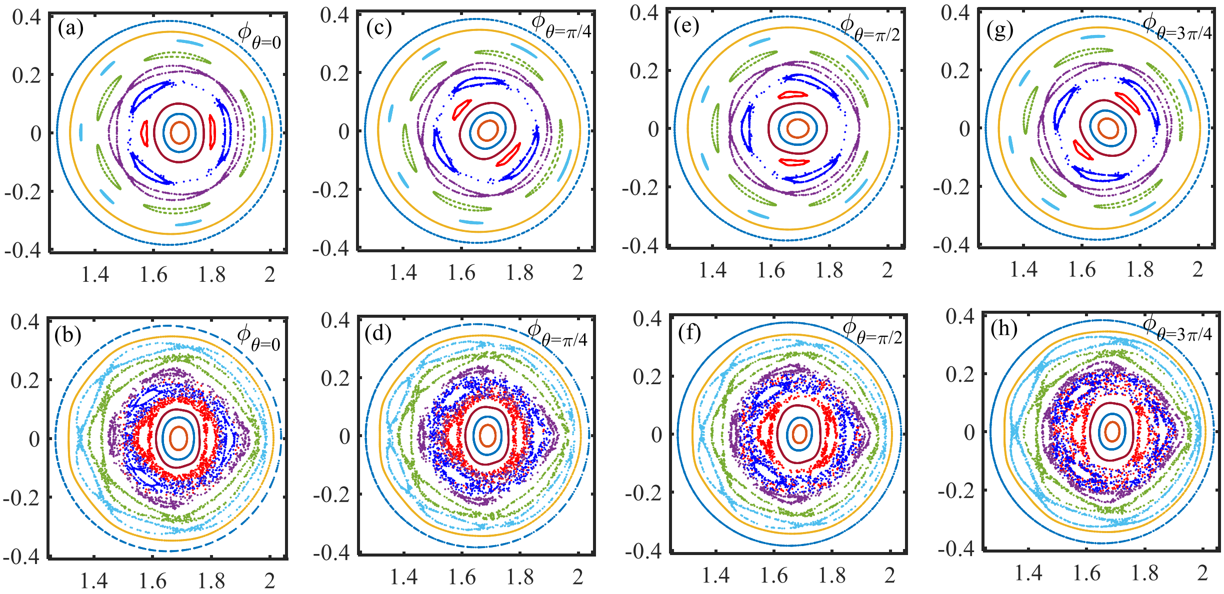

Fig. 3. Poincaré plots at the pellet injection time $t_1 \sim 5.2 \times 10^3\ \tau_A$ and at the time $t_3 \sim 1.25 \times 10^4\ \tau_A$, when the pellet crosses the q=2 rational surface, for different initial phases: (a–b) θ=0 (O-point of the magnetic island), (c–d) θ=π/4, (e–f) θ=π/2 (X-point of the magnetic island), and (g–h) θ=3π/4, at the same cross section of pellet injection.

It can be clearly understood that, the pellet ablation generates a local density perturbation as a delta function: $\tilde{\rho} = \rho_c \delta(\boldsymbol{r} - \boldsymbol{r}_{pellet})$, and in the cylinder coordinate this perturbation can be expansion into Fourier series: $\tilde{\rho} = \sum_{m,n} A_i(\psi) \exp[i(m\theta - n\xi + \phi)]$, including all the Fourier modes with different poloidal and toroidal mode numbers, so the density perturbation increases linearly. As the pellet continuously ablates and discharges plasma, the density perturbation of TM and the drift-like motion mode are linearly superposed. And the density distribution will generate diamagnetic and electric drift, and propagate into the drift-like motion mode with velocity structure. The velocity can generate magnetic field perturbation by convective term that is: $\frac{\partial \mathrm{B}_1}{\partial \mathrm{t}} = \nabla \times (v_1 \times B_0)$, where v_1 and B_0 are the velocity and magnetic field perturbations driven by the drift motion. It will make the magnetic island rotate in the poloidal direction and propagate in the radial direction by magnetic tension, so the magnetic island near the core region will adjust its phase to make the O-point face the pellet before it arrives.

References

[1] F.C. Schüller, Plasma Phys. Control. Fusion 37, A135-A162 (1995)

[2] T.C. Hender, J.C. Wesley, J. Bialek et al, Nucl. Fusion 47, S128-S202 (2007)

[3] D. Shiraki, N. Commaux, L.R. Baylor et al, Phys. Plasmas 23, 062516 (2016)

[4] Y. Li, Z.Y. Chen, W. Yan et al, Nucl. Fusion 61, 126025 (2021)

[5] L.R. Baylor, S.J. Meitner, T.E. Gebhart et al, Nucl. Fusion 59, 066008 (2019)